



Original contribution

Novel and established *EWSR1* gene fusions and associations identified by next-generation sequencing and fluorescence in-situ hybridization ^{☆,☆☆}



Melissa Krystel-Whittemore MD¹, Martin S. Taylor MD PhD¹, Miguel Rivera MD, Jochen K. Lennerz MD PhD, Long P. Le MD PhD, Dora Dias-Santagata PhD, Anthony John Iafrate MD PhD, Vikram Deshpande MD, Ivan Chebib MD, Gunlaugur Petur Nielsen MD, Chin-Lee Wu MD PhD, Valentina Nardi MD*

Massachusetts General Hospital, Department of Pathology, and Harvard Medical School, Boston, MA, 02114, USA

Received 19 June 2019; revised 6 August 2019; accepted 7 August 2019

Keywords:

Molecular pathology;
Next-generation sequencing;
FISH;
EWSR1

Summary *EWSR1* is a ‘promiscuous’ gene that can fuse with many different partner genes in phenotypically identical tumors or partner with the same genes in morphologically and behaviorally different neoplasms. Our study set out to examine the *EWSR1* fusions identified at our institution over a 3-year period, using various methods, their association with specific entities and possible detection of novel partners and associations. Sixty-three consecutive cases investigated for *EWSR1* gene fusions between 2015 and 2018 at our institution were included in this study. Fusions were identified by either break-apart fluorescence in-situ hybridization (FISH), our clinical RNA-based assay for fusion transcript detection or both. Twenty-eight cases were concurrently tested by FISH and NGS, 24 were tested by FISH alone and 11 by NGS alone. Of the 28 cases with dual testing, 24 were positive by both assays for an *EWSR1* gene fusion, 3 cases were discordant with a positive FISH assay and a negative NGS assay, and 1 case was discordant with a negative FISH assay but a positive NGS assay. Three novel fusions were identified: a complex rearrangement involving three genes (*EWSR1/RBFOX2/ERG*) in Ewing sarcoma, a *EWSR1/TCF7L2* fusion in a colon adenocarcinoma, and a *EWSR1/TFEB* fusion in a translocation-associated renal cell carcinoma. Both colonic adenocarcinoma and renal cell carcinoma had not been previously associated with *EWSR1* rearrangements to our knowledge. In a subset of cases, detection of a specific partner had an impact on the histological diagnosis and patient management. In our experience, the use of a targeted NGS-based fusion assay is superior to *EWSR1* break-apart FISH for the detection of known and novel *EWSR1* rearrangements and fusion partners, particularly given the emerging understanding that distinct fusion partners result in different diseases with distinct prognostic and therapeutic implications.

© 2019 Elsevier Inc. All rights reserved.

1. Introduction

The gene encoding for the Ewing Sarcoma (EWS) RNA binding protein 1 (*EWSR1*) was identified by Delattre and colleagues in 1992 at the chromosome 22 breakpoint of the t(11;22)(q24;q12) translocation that characterizes Ewing

¹ These authors equally contributed to this manuscript.

[☆] Disclosure/Conflict of Interest: There are no funding sources to declare.

^{☆☆} Drs A John Iafrate and Long P. Le declare an interest through their partial ownership of Archer Diagnostics and their advisory roles for that company.

* Corresponding author at: 55 Fruit St. Warren 820A, Boston, MA 02114.

E-mail address: vnardi@partners.org (V. Nardi).

sarcoma [1]. The *EWSR1* gene contains a transcriptional activation domain (TAD) at the N-terminus (within the first 7 exons), an RNA binding domain encompassing exons 11, 12, and 13 and a Zinc finger domain towards the C-terminus, and it encodes for a transcriptional regulator.

EWSR1 rearrangements occur in a variety of malignancies, as well as benign tumors, and lead to formation of chimeric genes in which the *EWSR1* N-terminal transcriptional activation domain (exons 1–7, 1–8, 1–9 or 1–10) is fused to the C-terminal DNA-binding domain of the partner gene, usually a transcription factor [2–6]. The transcriptional activation domain is a classically unstructured region now thought to function through phase-separation, forming local condensates and recruiting the Mediator coactivator to activate transcription at genomic loci specified by the fused DNA-binding domain [7,8].

Although most commonly rearranged in Ewing sarcoma, with the ETS (E twenty-six) transcription factors *FLI1* or *ERG*, the spectrum of *EWSR1*-rearranged neoplasms now includes many soft tissue tumors and even epithelial tumors, including desmoplastic small round cell tumor (*EWSR1/WT1*), clear cell sarcoma, hyalinizing clear cell carcinoma, and clear cell odontogenic carcinoma (*EWSR1/ATF1*), extraskeletal myxoid chondrosarcoma (*EWSR1/NR4A3*), myxoid liposarcoma (*EWSR1/DDIT3*), angiomatoid fibrous histiocytoma (*EWSR1/CREB1*), myoepithelial carcinoma (*EWSR1/PBX1*, *EWSR1/ZNF444*) [9], primary pulmonary myxoid sarcoma [10], and, rarely, low-grade fibromyxoid sarcoma [11] and sclerosing epithelioid fibrosarcoma [12–18]. Translocations involving *EWSR1* with specific partner genes are often not unique to specific tumor entities and morphologically identical tumors may be characterized by different *EWSR1* gene fusions [1].

Currently, RT-PCR and *EWSR1* break-apart FISH are the most commonly used assays to detect *EWSR1* rearrangements. Break-apart FISH is more widely available, requires a small amount of tissue (50 tumor cells in our laboratory), has a fast turnaround time, and is agnostic to the translocation partner. However, *EWSR1* break-apart FISH can be particularly challenging as the tissue can be crushed and the signals stretched. Intrachromosomal rearrangements are often undetectable. Additionally, the assay does not provide any information on the translocation partner. RT-PCR requires a priori knowledge of the translocation partners and high-quality RNA which is not always obtainable from formalin-fixed paraffin embedded (FFPE) specimens.

In 2015, we launched a targeted next-generation sequencing (NGS) fusion assay (Solid Fusion Assay (SFA) version 1, then replaced by a larger panel in version 2 and a sarcoma specific panel), which allowed us to identify specific fusion partners in *EWSR1* gene rearrangements. Briefly, this assay is based on anchored multiplex PCR (AMP) for the detection of targeted fusion transcripts and is optimized to work on FFPE-derived, variably degraded RNA [19]. Here we describe our 3-year experience using FISH and NGS to identify *EWSR1* fusions, including novel ones and novel disease associations.

2. Materials and methods

2.1. Patients and specimens

We searched internal databases per an IRB approved protocol for consecutive specimens tested by *EWSR1* FISH and/or an NGS fusion assay for *EWSR1* rearrangements from 2015 to 2018, the time both assays were clinically available. FISH and NGS were performed from formalin-fixed paraffin-embedded (FFPE) tissue blocks. Clinical information retrieved included patient age, sex, tumor site, tumor size, histologic diagnoses, and molecular diagnoses.

2.2. Immunohistochemistry

Standard staining protocols were used for beta-catenin (Leica Biosystems; Wetzlar, Germany) and TFEB immunohistochemical staining (Bethyl Laboratories; Montgomery, TX). Beta-catenin nuclear, but not membranous staining indicates activation of Wnt pathway usually through *CTNNB1* or *APC* mutations. Positive TFEB immunohistochemical staining demonstrates strong nuclear staining.

2.3. *EWSR1* FISH testing

EWSR1 FISH was performed on 5 µm sections from formalin-fixed paraffin-embedded tissue blocks using an Abbott Vysis (Abbott Laboratories, Abbott Park, IL; USA) *EWSR1* break-apart probe. This assay contains an orange 497 kb DNA probe and a green 1.1 Mb DNA probe, which flank the 5' and 3' ends respectively of the *EWSR1* gene on chromosome 22. *EWSR1* fusion positive cases showed splitting of the orange and green probe signals of a distance larger than the length of two probes, or isolated orange or green signals in addition to the normal orange-green un-split pair (presumed to represent an *EWSR1* rearrangement as previously reported [20]) in at least 8/50 scored tumor nuclei based on our assay validation.

2.4. *EWSR1* Fusion Transcript Identification using next-generation sequencing

The clinically validated next-generation sequencing (NGS)-based targeted fusion assays (Solid Fusion Assay v1 and 2, and Sarcoma Fusion Assay) [Supplemental File 1] requires RNA which is extracted as total nucleic acid from FFPE material (Formapure RNA Isolation, Agencourt AMPure; Beckman Coulter Life Sciences, Indianapolis, IL; USA). Double-stranded cDNA is synthesized, end-repaired, adenylated, and ligated with a half-functional adapter. Two hemi-nested PCR reactions using custom ArcherDx (Boulder, CO; USA) primers are performed to enrich for the targets of interest (specific genes/exons). These are then sequenced via Illumina MiSeq or NextSeq and aligned to the hg19 human

genome reference using bwa-mem [21]. A laboratory-developed algorithm is then used to detect and annotate fusion transcripts. The average analytic sensitivity of detecting mutations in this assay has been established in our laboratory at approximately 5% mutant allele [19].

3. Results

In total, there were 63 specimens with *EWSR1* fusions identified by either FISH, NGS, or both. This included 34 (54%) soft tissue lesions, 12 bone lesions (19%), and 17 lesions (27%) involving other tissues (salivary gland, orbit, pancreas, tongue, lung/bronchus, brain, colon/small bowel, kidney, and vagina).

Since 2015, we had 52 FISH cases (from 48 patients) positive for an *EWSR1* rearrangement. Of these, the 24 samples tested only by FISH included the following diagnoses: Ewing sarcoma (18 cases, 76%), extraskeletal myxoid chondrosarcoma (2 cases, 8%), *EWSR1* rearranged cutaneous myoepithelial tumor, clear cell sarcoma-like tumor of the gastrointestinal tract, desmoplastic small round cell tumor, and clear cell sarcoma of soft tissue (1 case each, 4%). During this time, our in-house NGS based targeted fusion assays (SFAv1, then SFAv2 and Sarcoma Fusion Assay), detected 36 *EWSR1* fusions (Figs. 1 and 2, Table 1). Twenty-eight samples had concurrent NGS and FISH testing: of these, 24 (86%) were positive for *EWSR1* fusion by both assays, 3 (11%) were *EWSR1* FISH positive and NGS negative, and 1 (3%) was FISH negative and NGS positive (Table 2). Using FISH as the gold-standard, the NGS assay had a sensitivity for *EWSR1* fusion detection of 89% and a positive predictive value of 96%. As we did not include “true negatives” in this study (FISH negative cases for which we had concurrent NGS results- the exception being the one case with negative FISH and positive NGS result, which was a false negative FISH case, described below-), we cannot calculate the specificity and negative predictive value of NGS versus FISH. Nevertheless, this NGS assay was negative for *EWSR1* fusions on

>2000 solid tumor specimens that were tested between 2015 and 2018. Although we did not perform *EWSR1* FISH on these specimens, they included tumors never reported to be associated with *EWSR1* rearrangements and in the majority of cases our targeted DNA or RNA sequencing assays detected oncogenic driver mutations mutually exclusive with *EWSR1* rearrangements. Therefore, our data suggests that NGS has very high specificity and negative predictive value in regard to *EWSR1* fusions.

The most commonly identified gene fusion was *EWSR1/FLII* (n = 13) followed by *EWSR1/CREB1* (n = 5). Four of the *EWSR1* fusions were seen in carcinomas (hyalinizing clear cell carcinomas, colon adenocarcinoma, and translocation associated renal cell carcinoma), while the other 32 fusions were seen in mesenchymal or glial tumors (Table 1, Figs. 1-3). Many of the *EWSR1* fusions identified in mesenchymal tumors have been previously described [9,12]. Besides *FLII* and *CREB1*, the additional fusion partners we detected by NGS included: *ATF1*, in hyalinizing clear cell carcinoma; *CREB3L1*, in sclerosing epithelioid fibrosarcoma; *ERG*, in Ewing sarcoma; *PBX2*, in myoepithelial carcinoma; *ZNF444*, in Ewing-like round cell sarcoma; *NFATC2*, in an emerging class of round cell sarcoma (manuscript submitted by Diaz-Perez J. A., et al); *NR4A3*, in extraskeletal myxoid chondrosarcoma; and *WT1*, in desmoplastic small round cell tumor. In addition, an *EWSR1/PATZ1* fusion, which has been previously described in high-grade gliomas [22], was identified in a pleomorphic xanthoastrocytoma.

Three novel fusions were identified: *EWSR1/RBFOX2/ERG*, *EWSR1/TCF7L2*, and *EWSR1/TFEB*. To further examine the *EWSR1/TCF7L2* and *EWSR1/TFEB* fusions, immunohistochemistry was performed (Fig. 4). We examined beta catenin immunohistochemistry in the *EWSR1/TCF7L2* translocated colon adenocarcinoma to rule out Wnt pathway activation through a mutation in *CTNNB1* or *APC*. The strong membranous and negative nuclear beta catenin staining seen in our case supports that the fusion is activating the relevant Wnt targeted genes directly by binding to the critical promoters and not through mutations in *APC* or *CTNNB1*. We used *TFEB* immunohistochemistry in our *EWSR1/TFEB*

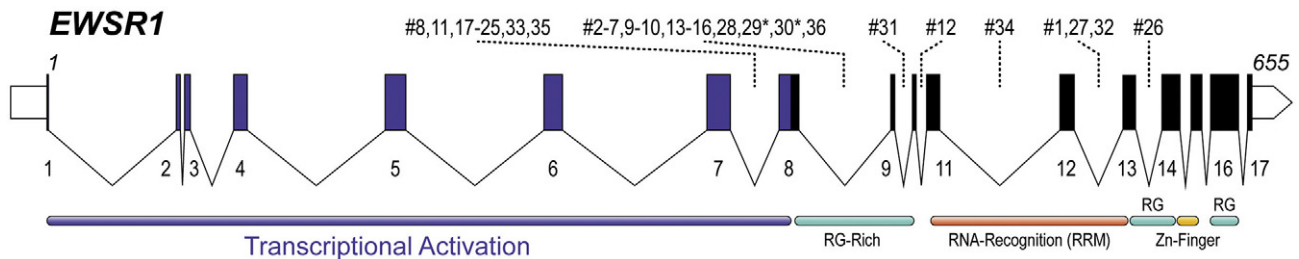
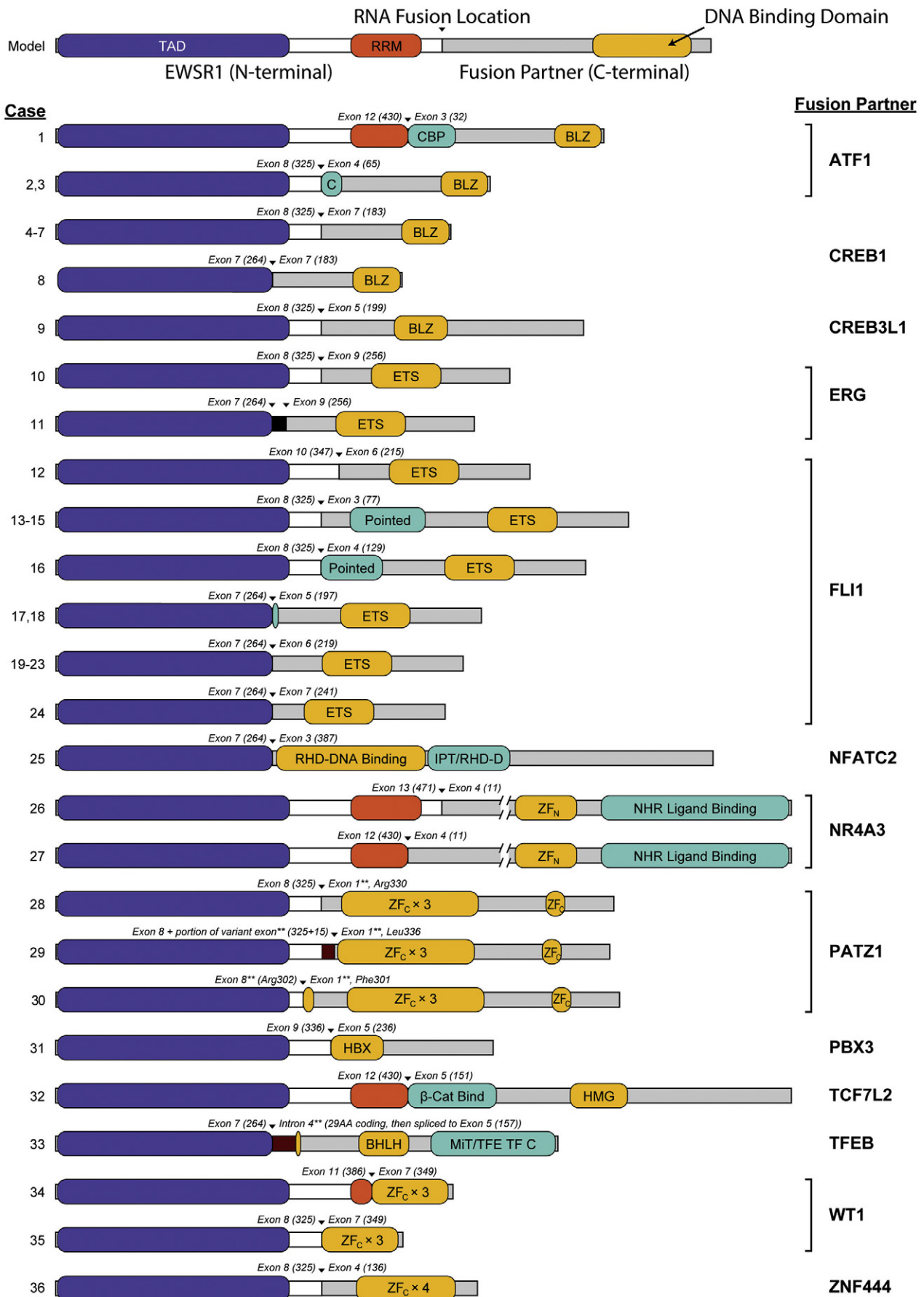


Fig. 1 Schematic of the *EWSR1* locus. Exons from transcript variant 3 (RefSeq NM_001163285.1). Fusion breakpoints for the indicated cases are shown: Cases 29 and 30 have exonic breakpoints (*); all others are intronic. Note that introns are drawn at a smaller scale than exons (30% scale, *EWSR1* locus is ~31.5 kB). Transcriptional activation domain is highlighted in blue. RG or RG-Rich: arginine/glycine rich domain; Zn-Finger: RanBP2-type zinc finger.



fusion case, which showed positive nuclear staining, consistent with TFEB overexpression seen in translocation-associated renal cell carcinomas.

Identification of the *EWSR1* rearrangement and fusion partner by NGS changed the histological diagnosis in seven cases (Table 3). In the *EWSR1/RBFOX2/ERG* rearranged Ewing sarcoma (Case 11), the *EWSR1/FLI1* rearranged adamantinoma-like Ewing sarcoma (Case 13), and the *EWSR1/NFATC2* rearranged round cell sarcoma (Case 25), the change in diagnosis affected clinical decision making and treatment choice.

Of the 3 FISH positive NGS negative cases, one was a lung adenocarcinoma, and the FISH results most likely represented a false positive, given the tumor histology and the numerous copy number changes detected by a DNA-based NGS assay in the *NKX2*, *MAP3K1*, *MYC*, *CCND2*, *CDK4*, *EBB3*, and *SRC* genes, respectively, on chromosomes 5, 12, 14, and 19, with the majority of copy number changes occurring in chromosome 12 (data not shown). Additionally, this tumor had several somatic mutations in *ARID1A*, *EGFR* (*c.2255C > G*), *ATM*, *BRCA2*, *BRCA1*, *TP53*, *CDH1*, and *CIC*. The other two cases, a poorly differentiated squamous cell carcinoma and a low-grade polypoid spindle cell neoplasm with angiomatous features, were also more likely to be a false positive FISH result given the tumor histology than a false negative NGS result due to a complex or unusual rearrangement. Furthermore, for the low-grade polypoid spindle cell neoplasm, the number of tumor nuclei showing split signals was very close to the cutoff of 15% (8.5/50 positive splits). The NGS positive, FISH negative case resulting from a complex *EWSR1/RBFOX2/ERG* three-way fusion was confirmed by RT-PCR with primers for *EWSR1* and *ERG* (data not shown).

4. Discussion

EWSR1 gene rearrangements are oncogenic drivers of a variety of mesenchymal and epithelial malignancies. Diagnosing these entities requires identification of an *EWSR1* rearrangement. At times, knowing also the *EWSR1* fusion partner leads to a specific diagnosis which could not be otherwise reached

by morphology and immunophenotype alone. We assessed the utility in our laboratory, a tertiary care center, of using *EWSR1* break-apart FISH and an NGS-based targeted fusion assay in detecting *EWSR1* gene rearrangements. The overall concordance between the two assays was 84%, although this is likely underestimated because the three discordant FISH positive NGS negative cases are likely false positive FISH results as described above, and accordingly the concordance may be better stated as 96% (24/25 cases). Furthermore, the NGS assay can be helpful in identifying false-positive FISH results.

We identified three novel fusions and novel associations. The complex *EWSR1/RBFOX2/ERG* fusion t(22;22;21) represents a variant of the canonical *EWSR1/ERG* rearrangement as it maintains the transcriptional activation domain of *EWSR1* and the DNA binding domain of *ERG*, adding 17 amino acids of coding sequence derived from *RBFOX2* exon 2 between *EWSR1* and *ERG*. Additionally, we detected a *EWSR1/TCF7L2* fusion in a colonic adenocarcinoma which shows, to our knowledge for the first time, an *EWSR1* rearrangement in this tumor type. *TCF7L2* fusions with other partners have been described in colonic adenocarcinoma [23]. *TCF7L2* encodes the TCF4 transcription factor which dimerizes with β -catenin and activates Wnt signaling. Aberrant Wnt activation is nearly ubiquitous in colorectal carcinoma, most commonly through mutations in *APC*, *CTNNB1* or *RNF43*, or through R-spondin fusions [24,25]. Translocations affecting *TCF7L2/TCF4* have been identified in colorectal carcinoma and proposed to be involved in aberrant β -catenin signaling [26], but the relevance of these translocations has been challenged due to their identification in normal tissues [23]. Unlike previously published *TCF7L2* translocations to partners of unclear function, our case follows the paradigm of *EWSR1* fusions, joining the transcriptional activation domain of *EWSR1* to the DNA binding domain of *TCF7L2*. We conclude these data are supportive of a novel mechanism (*EWSR1/TCF7L2* fusion) for activation of the Wnt signaling pathway in colon adenocarcinoma, which is supported by negative nuclear beta catenin staining on immunohistochemical staining, ruling out mutations in *CTNNB1* or *APC*.

Fig. 2 *EWSR1* fusion positive cases with breakpoint location and fusion product. Schematic of a model *EWSR1* fusion (top row) and predicted fusion protein products (bottom, see also Table 1). All cases fuse the N-terminal transcriptional activation domain (TAD) of *EWSR1* (purple boxes) to a partner with a DNA binding domain (yellow boxes). Triangles and Exon notation indicate the fusion breakpoints; ** indicate cases with exonic breakpoints (cases 28–30) or an intronic breakpoint with coding sequence derived from the intron (case 33). Maroon boxes indicate coding sequence derived from a portion of an alternate exon (case 30), or an intron (case 33). Case 11 is a complex rearrangement t(22;22;21) *EWSR1-RBFOX2-ERG* with two breakpoints (triangles) identified and includes 17 amino acids of coding sequence derived from *RBFOX2* exon 2, but in an alternate reading frame (black bar). Yellow shaded boxes mark DNA binding domains (BLZ: basic-leucine zipper; ETS: erythroblast transformation specific; RHD-DNA Binding: Rel homology domain, DNA binding subdomain; ZF_N: zinc finger, nuclear hormone receptor type; ZF_C: zinc finger, C2H2 type; HBX: homeobox domain; HMG: high mobility group box domain; BHLH: basic helix loop helix). Turquoise and orange boxes are other major annotated sequence features (RRM: *EWSR1* RNA recognition motif; Co-CBP/CBP: Coactivator CBP binding domain; Pointed: sterile alpha motif (SAM) / helix loop helix (HLH) oligomerization domain; IPT/RHD-Dimer: IPT (Ig-like, plexin, transcription factor) DNA binding and Rel homology dimerization domain; NHR ligand binding: nuclear hormone receptor ligand binding; MiT/TFE TF C-Term: MiT/TFE transcription family C-terminal domain). Proteins are drawn to scale (*EWSR1/TCF7L1* fusion = 898 AA); breaks in *NR4A3* hide 114 AA and 73 AA respectively in Cases 26 and 27 (*EWSR1-NR4A3* fusions, 1012AA and 971AA, respectively).

Table 1 *EWSR1* fusions identified by NGS Solid Fusion Assay with FISH concordance

Study number	Age (years)	Sex	Tumor site	Left Partner Gene	Break point 1	Right Partner Gene	Break point 2	Diagnosis	<i>EWSR1</i> FISH
1	46	F	Salivary gland	<i>EWSR1</i>	Exon 12	<i>ATF1</i>	Exon 3	Hyalinizing clear cell carcinoma	NA
2	47	F	Tongue	<i>EWSR1</i>	Exon 8	<i>ATF1</i>	Exon 4	Hyalinizing clear cell carcinoma	C
3	29	F	Orbit	<i>EWSR1</i>	Exon 8	<i>ATF1</i>	Exon 4	Clear cell sarcoma	NA
4	60	F	Mediastinal mass	<i>EWSR1</i>	Exon 8	<i>CREB1</i>	Exon 7	Angiomatoid fibrous histiocyoma	C
5	17	F	Anterolateral knee soft tissue	<i>EWSR1</i>	Exon 8	<i>CREB1</i>	Exon 7	Angiomatoid fibrous histiocyoma	C
6	55	F	Hip soft tissue	<i>EWSR1</i>	Exon 8	<i>CREB1</i>	Exon 7	Angiomatoid fibrous histiocyoma	C
7	10	M	Medial arm mass	<i>EWSR1</i>	Exon 8	<i>CREB1</i>	Exon 7	Angiomatoid fibrous histiocyoma	C
8	15	F	Upper arm soft tissue	<i>EWSR1</i>	Exon 7	<i>CREB1</i>	Exon 7	Angiomatoid fibrous histiocyoma	C
9	76	F	Lung	<i>EWSR1</i>	Exon 8	<i>CREB3L1</i>	Exon 5	Sclerosing epithelioid fibrosarcoma	C
10	NP	NP	NP	<i>EWSR1</i>	Exon 8	<i>ERG</i>	Exon 9	Ewing sarcoma	NA
11	7	M	Mandible soft tissue	<i>EWSR1</i>		<i>RBFOX2/ERG</i>		Ewing sarcoma ^a	D ^b
12	49	F	Chest wall	<i>EWSR1</i>	Exon 10	<i>FLI1</i>	Exon 6	Ewing sarcoma	NA
13	41	M	Salivary gland	<i>EWSR1</i>	Exon 8	<i>FLI1</i>	Exon 3	Adamantinoma-like Ewing sarcoma (AES) ^a	C
14	28	M	Iliac	<i>EWSR1</i>	Exon 8	<i>FLI1</i>	Exon 3	Ewing sarcoma	C
15	4	M	Nasal soft tissue	<i>EWSR1</i>	Exon 8	<i>FLI1</i>	Exon 3	Ewing sarcoma	C
16	22	F	Lung (metastatic from pelvic soft tissue)	<i>EWSR1</i>	Exon 8	<i>FLI1</i>	Exon 4	Ewing sarcoma	NA
17	21	F	Rib	<i>EWSR1</i>	Exon 7	<i>FLI1</i>	Exon 5	Ewing sarcoma	C
18	59	F	Pancreas	<i>EWSR1</i>	Exon 7	<i>FLI1</i>	Exon 5	Adamantinoma-like Ewing sarcoma (AES)	NA
19	21	F	Groin soft tissue	<i>EWSR1</i>	Exon 7	<i>FLI1</i>	Exon 6	Ewing sarcoma	C
20	19	M	Spinal cord	<i>EWSR1</i>	Exon 7	<i>FLI1</i>	Exon 6	Ewing sarcoma	NA
21	14	M	Forearm	<i>EWSR1</i>	Exon 7	<i>FLI1</i>	Exon 6	Ewing sarcoma	C
22	55	F	Pelvic soft tissue	<i>EWSR1</i>	Exon 7	<i>FLI1</i>	Exon 6	Ewing sarcoma	C
23	34	M	L5-S1 mass	<i>EWSR1</i>	Exon 7	<i>FLI1</i>	Exon 6	Ewing sarcoma	NA
24	12	M	Chest wall	<i>EWSR1</i>	Exon 7	<i>FLI1</i>	Exon 7	Ewing sarcoma	NA
25	46	M	Distal femur	<i>EWSR1</i>	Exon 7	<i>NFATC2</i>	Exon 3	Malignant myoepithelioma ^a	C
26	71	M	Thigh soft tissue	<i>EWSR1</i>	Exon 13	<i>NR4A3</i>	Exon 4	Extraskeletal myxoid chondrosarcoma	C
27	77	M	Epigastric abdominal wall	<i>EWSR1</i>	Exon 12	<i>NR4A3</i>	Exon 4	Extraskeletal myxoid chondrosarcoma	C
28	31	F	Retroperitoneal soft tissue	<i>EWSR1</i>	Exon 9	<i>PATZ1</i>	Exon 1	<i>EWSR1-PATZ1</i> spindle and round cell sarcoma ^a	C
29	53	F	Pelvic sidewall	<i>EWSR1</i>	Exon 9	<i>PATZ1</i>	Exon 1	<i>EWSR1-PATZ1</i> spindle and round cell sarcoma ^a	C
30	36	F	Brain	<i>EWSR1</i>	Exon 9	<i>PATZ1</i>	Exon 1	Pleomorphic xanthoastrocytoma	C
31	58	M	Calf soft tissue	<i>EWSR1</i>	Exon 9	<i>PBX3</i>	Exon 5	Malignant myoepithelioma	NA
32	62	M	Colon	<i>EWSR1</i>	Exon 12	<i>TCF7L2</i>	Exon 5	Colon adenocarcinoma	C
33	25	F	Kidney	<i>EWSR1</i>	Exon 7	<i>TFEB</i>	Intron 4	Translocation associated renal cell carcinoma	NA
34	39	M	Intraabdominal soft tissue	<i>EWSR1</i>	Exon 11	<i>WT1</i>	Exon 8	Desmoplastic small round cell tumor	C
35	38	F	Pelvic and abdominal soft tissue mass	<i>EWSR1</i>	Exon 7	<i>WT1</i>	Exon 8	Desmoplastic small round cell tumor ^a	C
36	44	F	Left flank mass	<i>EWSR1</i>	Exon 8	<i>ZNF444</i>	Exon 5	Ewing-like round cell sarcoma (<i>EWSR1/ZNF444</i> fusion positive sarcoma) ^a	C

Abbreviations: C=, concordant; D, discordant; NA, not available;

F, female; M, male; NP, not provided.

^a Detection of a specific partner had impact on histologic diagnosis.

^b False-negative FISH result.

Table 2 Concordance between FISH and NGS assays for detection of *EWSR1* rearrangements

	FISH positive	FISH negative
NGS fusion assay positive	24/28 (86%)	1/28 (3%)
NGS fusion assay negative	3/28 (11%)	0/28 (0%)

Finally, we identified a *EWSR1/TFEB* fusion in a translocation-associated renal cell carcinoma, defined by having rearrangements of either the *TFE3* or *TFEB* genes [27]. *TFE3* and *TFEB* are members of the microphthalmia-associated transcription (MiT) family of transcription factors which regulates melanocyte and osteoclast differentiation [28]. In this case, the *EWSR1* N-terminal transcriptional activation domain was translocated to *TFEB* as the transcription factor fusion partner. Fusions involving *TFE3* or *TFEB* in translocation-associated renal cell carcinomas result in protein overexpression and nuclear staining with antibodies for, respectively *TFE3* and *TFEB*, which was demonstrated in our tumor. In our case, *EWSR1* appears as a novel partner of *TFEB* and, to our knowledge, *EWSR1* fusions have not been described in renal cell carcinomas.

In 6 cases, in which the histological diagnosis was not entirely clear, the final diagnosis was reached only upon detection of a *EWSR1* rearrangement and upon identification of its

fusion partner by the NGS assay (Table 3). The detection of *EWSR1/ZNF444* in case 30 is interesting, in that *EWSR1/ZNF444* has been described in myoepithelial carcinoma and tumors, but not in sarcomas. This case specifically did not fit the immunophenotype of myoepithelial carcinoma, and overall the diagnosis of sarcoma was favored. *EWSR1/ZNF444* fusion positive sarcomas may be a distinct entity similarly to the *EWSR1/PATZ1* spindle and round-cell sarcoma [29].

In two of these cases, clinical treatment was managed differently upon the identification of an Ewing sarcoma associated *EWSR1* fusion: the detection of the *EWSR1/RBFOX2/ERG* fusion in a mandible tumor allowed to make the diagnosis of Ewing sarcoma instead of lymphoblastic lymphoma versus malignant round cell neoplasm and detection of the *EWSR1/FLI1* fusion in the parotid tumor changed the diagnosis from high-grade, poorly differentiated carcinoma to that of adamantinoma-like Ewing sarcoma. In these cases, the diagnosis of Ewing sarcoma would not have been established without the identification of the rearrangement and of the specific fusion partner, which led to a change in prognosis and clinical management.

Finally, detection of the fusion partner gene *PATZ1* led to recognition of a new association with lower grade brain tumors and of the new entity of *EWSR1/PATZ1* spindle and round cell sarcoma [22,29], which may have a different biology and clinical course and may require different treatment.

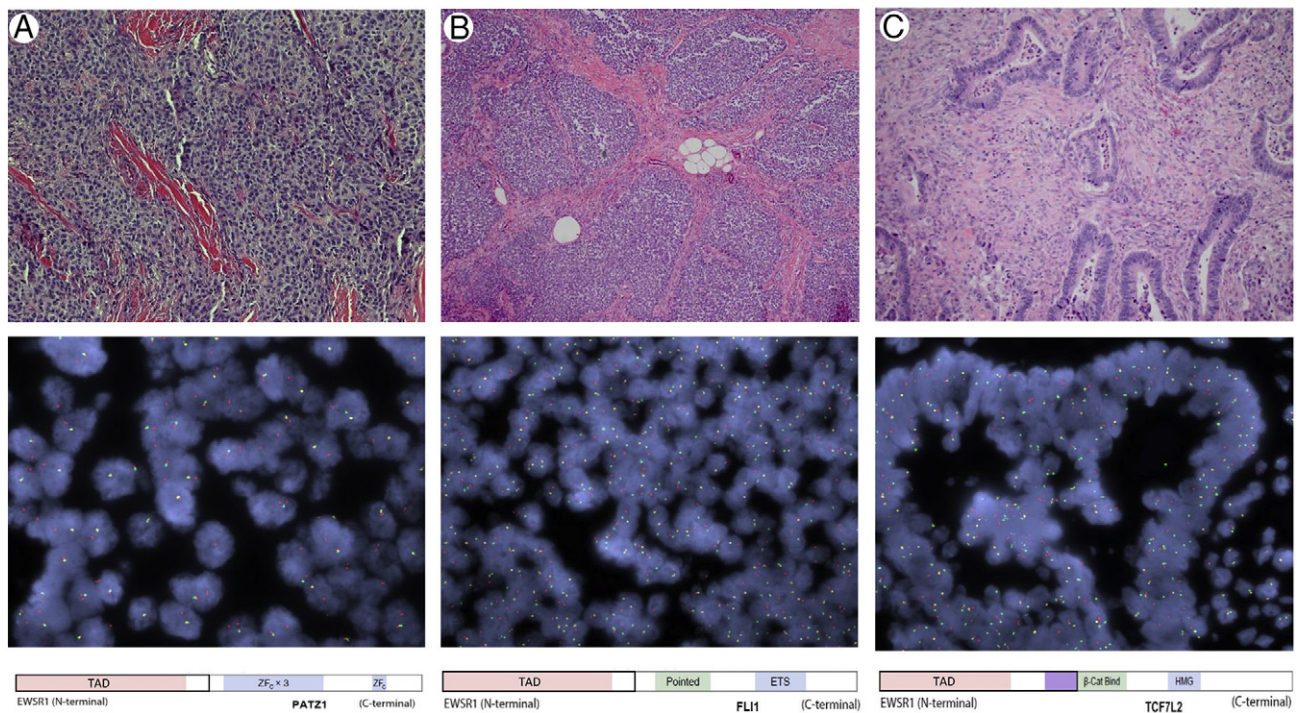


Fig. 3 Selected cases showing unexpected *EWSR1* fusions (H&E, FISH, and Fusion Diagram). (A) *EWSR1/PATZ1* rearrangement in a spindle and round cell sarcoma of the retroperitoneum, a subset of round cell sarcomas in which this fusion is associated with rhabdomyoblastic differentiation. (B) *EWSR1/FLI1* fusion changed the diagnosis to adamantinoma-like Ewing sarcoma (AES) of the parotid gland. (C) *EWSR1/TCF7L2* fusion is the first reported *EWSR1* rearrangement in a colonic adenocarcinoma. (TAD: Transcriptional activation domain; ZF₂: zinc finger; ETS: erythroblast transformation specific; β-cat: Beta catenin; HMG: high mobility group box domain).

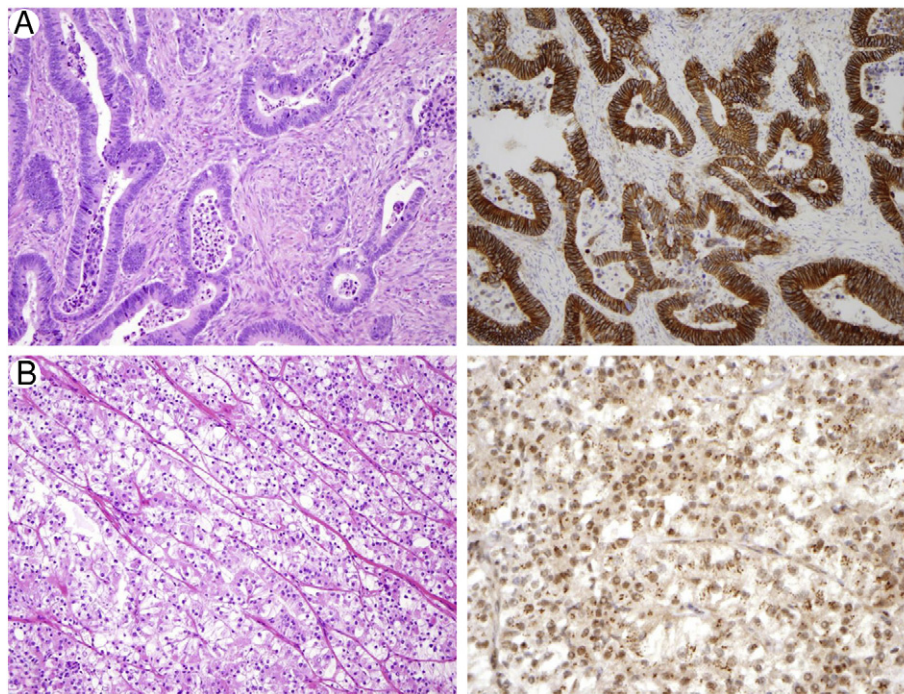


Fig. 4 Immunohistochemistry of beta-catenin (A) and TFEB (B) in *EWSR1* translocated tumors. (A) H&E of colon adenocarcinoma with *EWSR1/TCF7L2* fusion demonstrating strong cytoplasmic beta-catenin staining with absence of nuclear staining on IHC. (B) H&E of *TFEB* translocation-associated renal cell carcinoma with *EWSR1/TFEB* fusion demonstrating nuclear TFEB staining on IHC.

Table 3 Clinical impact of identification of *EWSR1* fusion partners

Study no.	Original diagnosis	<i>EWSR1</i> fusion partner	Final diagnosis	Treatment change
11	Lymphoblastic lymphoma versus malignant round cell neoplasm	<i>RBFox2/ERG</i>	Ewing sarcoma	Yes
13	Poorly differentiated carcinoma	<i>FLI1</i>	Adamantinoma-like Ewing sarcoma	Yes
25	Malignant round cell tumor vs. myoepithelial carcinoma	<i>NFATC2</i>	<i>EWSR1/NFATC2</i> round cell sarcoma	Yes
28	High grade sarcoma	<i>PATZ1</i>	<i>EWSR1/PATZ1</i> spindle and round-cell sarcoma	No
29	High grade spindle and epithelioid cell sarcoma with rhabdomyoblastic differentiation	<i>PATZ1</i>	<i>EWSR1/PATZ1</i> spindle and round-cell sarcoma	No
35	Malignant round cell tumor	<i>WT1</i>	Desmoplastic small round cell tumor	No
36	<i>EWSR1</i> translocated malignant small round blue cell tumor	<i>ZNF444</i>	Ewing-like round cell sarcoma	No

In conclusion, *EWSR1* break-apart FISH and a targeted NGS-based fusion assay complement each other in the detection of *EWSR1* fusions in a wide range of tumor types. However, NGS, although possibly less sensitive than FISH when RNA is degraded, has the advantage of providing more detailed information on exact fusion partners, which can help to better understand tumor biology, refine tumor classification and foster the development of novel therapeutics for *EWSR1* driven malignancies. For this reason, NGS proves to have added benefit to FISH in the diagnosis and understanding of *EWSR1* translocated tumors.

Supplementary data

Supplementary data to this article can be found online at <https://doi.org/10.1016/j.humpath.2019.08.006>.

Acknowledgment

We thank N. Bhatla for the original source code modified to make Fig. 1 (WormWeb.org).

References

- [1] Delattre O, Zucman J, Plougastel B, et al. Gene fusion with an ETS DNA-binding domain caused by chromosome translocation in human tumours. *Nature* 1992;359:162-5.
- [2] Ohno T, Rao VN, Reddy ES. EWS/Fli-1 chimeric protein is a transcriptional activator. *Cancer Res* 1993;53:5859-63.
- [3] Aman P, Panagopoulos I, Lassen C, et al. Expression patterns of the human sarcoma-associated genes FUS and EWS and the genomic structure of FUS. *Genomics* 1996;37:1-8.
- [4] Plougastel B, Zucman J, Peter M, Thomas G, Delattre O. Genomic structure of the EWS gene and its relationship to EWSR1, a site of tumor-associated chromosome translocation. *Genomics* 1993;18:609-15.
- [5] May WA, Gishizky ML, Lessnick SL, et al. Ewing sarcoma 11;22 translocation produces a chimeric transcription factor that requires the DNA-binding domain encoded by FLI1 for transformation. *Proc Natl Acad Sci* 1993;90:5752-6.
- [6] Li KK, Lee KA. Transcriptional activation by the Ewing's sarcoma (EWS) oncogene can be cis-repressed by the EWS RNA-binding domain. *J Biol Chem* 2000;275:23053-8.
- [7] Wang J, Choi JM, Holehouse AS, et al. A molecular grammar governing the driving forces for phase separation of prion-like RNA binding proteins. *Cell* 2018 Jul 26;174:688-699.e16.
- [8] Bojja A, Klein IA, Sabari BR, et al. Transcription factors activate genes through the phase-separation capacity of their activation domains. *Cell* 2018;175:1842-1855.e16.
- [9] Antonescu CR, Zhang L, Chang NE, et al. EWSR1-POU5F1 fusion in soft tissue myoepithelial tumors. A molecular analysis of sixty-six cases, including soft tissue, bone, and visceral lesions, showing common involvement of the EWSR1 gene. *Genes Chromosomes Cancer* 2010;49:1114-24.
- [10] Thway, et al. Evaluation of the optimal provision of formalin-fixed, paraffin-embedded material for reverse transcription-PCR in soft-tissue tumour diagnosis. *J Clin Pathol* 2017 Jan;70:20-4.
- [11] Lau, et al. EWSR1-CREB3L1 gene fusion: a novel alternative molecular aberration of low-grade fibromyxoid sarcoma. *Am J Surg Pathol* 2013 May;37:734-8.
- [12] Schaefer I, Cote G, Hornick J. Contemporary sarcoma diagnosis, genetics, and genomics. *J Clin Oncol* 2018;36:101-10.
- [13] Hart A, Melet F, Grossfeld P, et al. Fli-1 is required for murine vascular and megakaryocytic development and is hemizygously deleted in patients with thrombocytopenia. *Immunity* 2000;13:167-77.
- [14] Hossain A, Saunders GF. The human sex-determining gene SRY is a direct target of WT1. *J Biol Chem* 2001;276:16817-23.
- [15] Ficara F, Murphy MJ, Lin M, Cleary ML. Pbx1 regulates self-renewal of long-term hematopoietic stem cells by maintaining their quiescence. *Cell Stem Cell* 2008;2:484-96.
- [16] Weinreb I. Hyalinizing clear cell carcinoma of salivary gland: a review and update. *Head Neck Pathol* 2013;7(Suppl. 1):20-9.
- [17] Agaram NP, Zhang L, Sung YS, Singer S, Antonescu CR. Extraskelletal myxoid chondrosarcoma with non-EWSR1-NR4A3 variant fusions correlate with rhabdoid phenotype and high-grade morphology. *HUM PATHOL* 2014;45:1084-91.
- [18] Fisher C. The diversity of soft tissue tumours with EWSR1 gene rearrangements: a review. *Histopathology* 2014;64:134-50.
- [19] Zheng Z, Liebers M, Zhelyazhova B, et al. Anchored multiplex PCR for targeted next-generation sequencing. *Nat Med* 2014;20:1479-84.
- [20] Sankar S, Lessnick SL. Promiscuous partnerships in Ewing's sarcoma. *Cancer Genet* 2011;204:351-65.
- [21] Li H, Durbin R. Fast and accurate short read alignment with burrows-wheeler transform. *Bioinformatics* 2009;25:1754-60.
- [22] Johnson A, Severson E, Gay L, et al. Comprehensive genomic profiling of 282 pediatric low- and high-grade gliomas reveals genomic drivers, tumor mutational burden, and hypermutation signatures. *Oncologist* 2017; 22:1478-90.
- [23] Nome T, Hoff AM, Bakken AC, Rognum TO, Nesbakken A, Skotheim RI. High frequency of fusion transcripts involving *TCF7L2* in colorectal cancer: novel fusion partner and splice variants. *PLoS ONE* 2014;9: e91264.
- [24] Seshagiri S, Stawiski EW, Durinck S, et al. Recurrent R-spondin fusions in colon cancer. *Nature* 2012;488:660-4.
- [25] Novellasademunt L, Antas P, Li VS. Targeting Wnt signaling in colorectal cancer. A review in the theme: cell signaling: proteins, pathways and mechanisms. *Am J Physiol Cell Physiol* 2015;309:C511-21.
- [26] Bass AJ, Lawrence MS, Brace LE, et al. Genomic sequencing of colorectal adenocarcinomas identifies a recurrent VTI1A-TCF7L2 fusion. *Nat Genet* 2011;43:964-8 Published 2011 Sep 4 <https://doi.org/10.1038/ng.936>.
- [27] Zhong M, De Angelo P, Osborne L, et al. Translocation renal cell carcinomas in adults: a single institution experience. *Am J Surg Pathol* 2012; 36:654-62.
- [28] Inamura K. Translocation renal cell carcinoma: an update on Clinicopathological and molecular features. *Cancers (Basel)* 2017;9:111.
- [29] Chougule A, Taylor M, Nardi V, et al. Spindle and round cell sarcoma with EWSR1-PATZ1 gene fusion: a sarcoma with polyphenotypic differentiation. *Am J Surg Pathol* 2019 Feb;43:220-8.